

Characterization of the long-time and short-time predictability of low-order models of the atmosphere

R. Benzi¹, M. Marrocu², A. Mazzino³ and E. Trovatore⁴

¹ Autorità per l'Informatica nella Pubblica Amministrazione,
Via Solferino 15, I-00100 Roma, Italy.

² CRS4, C.P. 94, I-09010 Uta (Cagliari), Italy.

³ INFN–Dipartimento di Fisica, Università di Genova,
Via Dodecaneso 33, I-16146, Genova, Italy.

⁴ Centro Meteo–Idrologico della Regione Liguria,
Via Dodecaneso 33, I-16146, Genova, Italy.

Abstract

Methods to quantify predictability properties of atmospheric flows are proposed. The “Extended Self Similarity” (ESS) technique, recently employed in turbulence data analysis, is used to characterize predictability properties at short and long times. We apply our methods to the low-order atmospheric model of Lorenz (1980). We also investigate how initialization procedures that eliminate gravity waves from the model dynamics influence predictability properties.

1 Introduction

The behavior of a system such as the atmosphere cannot be predicted with prescribed spatial detail beyond a certain characteristic time because initially close trajectories diverge with time. Since the first systematic studies of error growth, low-order models of the atmospheric circulation, such as the Lorenz (1963,1980) models, have been used to study the predictability properties of chaotic systems in general and of the atmosphere in particular. In spite of their lack of realism, low order models can be still considered useful tools to study some of the mechanisms that limit predictability. Several different methods have been adopted in studies on the subject. In this paper we will follow the guidelines of methods employed in the theory of dynamical systems (Benzi *et al.* 1985;

Benzi and Carnevale 1989) in order to study the statistics of divergence of initially close forecasts.

As is well-known (Oseledec 1968), for chaotic systems the asymptotic divergence of initially close trajectories behave exponentially with a rate given by the maximum Lyapunov exponent λ_1 (Benettin *et al.* 1980). Lyapunov exponents are defined as global averages on the attractor of a chaotic system; however, predictability is a local property in the phase space. Indeed, operational forecasting experience indicates that the skill associated with individual forecasts may vary greatly. Thus, predictability properties of atmospheric models exhibit large variability in both time and phase space (Palmer *et al.* 1990); that is, predictability is characterized by the presence of fluctuations.

Another important point is the existence of a period of transient growth that can exceed the Lyapunov exponential growth rate (Mukougawa *et al.* 1991; Nicolis 1992; Trevisan 1993; Trevisan and Legnani 1995). Error amplification on short time scales is controlled by rapidly growing perturbations that are not of normal-mode form. If the normal modes of instability of a stationary solution are not orthogonal, perturbations may for some time grow faster than the most unstable normal mode and the global average growth rate of errors, initially in a random direction, attains the asymptotic value given by the first Lyapunov exponent after a finite period of time. The concept of transient enhanced exponential growth was introduced by Farrell (1985) and Lacarra and Talagrand (1988). A common application of this concept used in numerical weather prediction consists in finding the initial perturbation that grows fastest in a given period of time (ECMWF 1992; Mureau *et al.* 1993; Molteni *et al.* 1996).

In this paper we want to address the following questions:

- how can the fluctuations in the predictability properties of atmospheric models be described?
- how can the predictability properties in the transient region of super-exponential growth be described?
- what is the influence of initialization procedures on the predictability fluctuations?

Our major goal will be to give new insights on these three (related) problems. Specifically, we will use, for the first time in atmospheric science, mathematical tools which are well-known in the theory of dynamical systems and in other contexts (as in turbulence theory) and which allow the quantitative characterization of predictability fluctuations at long and short times.

The outline of the paper is as follows: in sec. 2, we discuss the mathematical background needed to describe the statistics of error growth. A quantitative definition of its statistical fluctuations (a characteristic also known as *intermittency*) is given in terms of an infinite set of characteristic time scales, related to the so-called generalized Lyapunov exponents $L(q)$. In the absence of fluctuations, the generalized Lyapunov exponents are linearly dependent on λ_1 , thus making the maximum Lyapunov exponent the only

relevant parameter defining the predictability. We also discuss how to characterize the predictability fluctuations at short times by means of new techniques recently applied in turbulence theory. In sec. 3, we apply these ideas to the low-order model introduced and studied by Lorenz (1980). In sec. 4 we investigate how predictability properties are modified by the superbalance equations introduced by Lorenz (1980), which do not support gravity wave oscillations. This allows us to make an assessment of the role played by gravity wave oscillations in enhancing predictability fluctuations at short times. Conclusions follow in sec. 5.

2 Predictability fluctuations: the general theory

In this section we shall review some basic mathematical definitions and concepts related to sensitive dependence of the trajectory of a generic dynamical system on initial conditions.

Let us consider an N -dimensional dynamical system given by the equations:

$$\dot{\mathbf{x}} = \mathbf{f}(\mathbf{x}), \quad (1)$$

where $\mathbf{x} \in R^N$. The time evolution of an infinitesimal disturbance $\delta\mathbf{x}(t)$ is given by the linearized equations:

$$\delta\dot{\mathbf{x}}(t) = \mathbf{Df} \delta\mathbf{x}(t), \quad (2)$$

where $\delta\mathbf{x}(0) \neq 0$ and $Df_{ij} = \left. \frac{\partial f_i}{\partial x_j} \right|_{\mathbf{x}=\mathbf{x}(t)}$.

We can define the response function $R(t, 0)$ as

$$R(t, 0) = \frac{|\delta\mathbf{x}(t)|}{|\delta\mathbf{x}(0)|}. \quad (3)$$

The Oseledec theorem (Oseledec 1968) tells us that, for $t \rightarrow \infty$ and for almost all (in the sense of measure theory) initial conditions $\delta\mathbf{x}(0)$, we have:

$$R(t, 0) \rightarrow e^{\lambda_1 t}, \quad (4)$$

where λ_1 is called the *maximum Lyapunov exponent* (Benettin *et al.* 1980). One may venture to guess that this exponential growth is valid even at finite times and that λ_1^{-1} is the only characteristic time scale of the error growth; however as is well-known, this

is not the case (see, for example, Trevisan and Legnani 1995). Indeed, even if t is large enough to allow the observation of an exponential growth rate of $R(t, 0)$, λ_1^{-1} is not the only relevant time scale: depending on the initial conditions, dynamical systems can show states or configurations that can be predicted for times longer or shorter than λ_1^{-1} .

The question we want to address is related to the existence of well-defined mathematical quantities able to characterize these predictability fluctuations in chaotic systems (Eckmann and Procaccia 1986; Paladin *et al.* 1986) and in particular in atmospheric models (Benzi and Carnevale 1989; Trevisan and Legnani 1995). This aspect will be investigated in sec. 2.1.

Another issue to address is that for times not long enough, the dynamical behavior of $R(t, 0)$ is not necessarily characterized by an exponential growth rate. This question has been investigated by Mukougawa *et al.* (1991), Nicolis (1992), and Trevisan (1993), Trevisan and Legnani (1995), amongst others, and turns out to be of great importance in realistic applications of predictability theory. We shall come to this question in sec. 2.2.

2.1 Characterization of predictability fluctuations at long times

In this section we recall the concept of generalized Lyapunov exponents, already introduced in atmospheric applications by Benzi and Carnevale (1989). We point out that λ_1 is an average quantity and we define the probability $P_t(\gamma)$ of having a local exponent γ different from λ_1 . Then we derive the relationships between all these quantities and we give two examples of simple probability density functions (p.d.f.'s). In particular, we show that the log-Poisson p.d.f, proposed here for the first time in a meteorological context, has some interesting features regarding the description of strong fluctuations.

2.1.1 Basic concepts

In this section we review some general statistical properties of the response function $R(t, 0)$ (see also Benzi and Carnevale 1989). Let us consider times long enough to have an exponential growth rate for the response function $R(t, 0)$. Let us introduce the quantities:

$$\langle R(t, 0)^q \rangle, \tag{5}$$

where $\langle \cdot \rangle$ is the average over different initial conditions.

If λ_1 were the only relevant time scale characterizing the error growth, then we should expect:

$$\langle R(t, 0)^q \rangle \sim e^{\lambda_1 q t}. \tag{6}$$

On the other hand, if many times scales characterize the error growth, we should have the more general behavior:

$$\langle R(t, 0)^q \rangle \sim e^{L(q)t}, \quad (7)$$

where the $L(q)$'s are the so-called *generalized Lyapunov exponents* (Fujisaka 1983; Benzi *et al.* 1985). In general, $L(q)$ is not a linear function of q .

Before explaining in detail the physical meaning of eq. (7), let us give simple examples of dynamical systems that satisfy either eq. (6) or eq. (7).

Let us consider the one dimensional ‘‘tent’’ map (see Fig. 1):

$$x_{n+1} = \begin{cases} x_n & (0 \leq x \leq c) \\ \frac{1-c-x_n}{1-c} & (c < x \leq 1). \end{cases} \quad (8)$$

In this case, $t = n$ is a discrete time and the corresponding response function $R(n, 0)$ is given by:

$$R(n, 0) = \prod_{i=1}^n D_i, \quad (9)$$

where D_i is given either by $1/c$ or $1/(1-c)$, depending on whether $x_i \in [0, c]$ or $x_i \in [c, 1]$, respectively.

In order to compute $\langle R(n, 0)^q \rangle$, we need to know the p.d.f. of x . For the tent map the p.d.f. is that of the uniform distribution on the interval $[0, 1]$ (Frisch 1995). It then follows from (9) that:

$$\begin{aligned} \langle R(n, 0)^q \rangle &= \left\{ \int_0^c \left[\frac{1}{c}\right]^q dx + \int_c^1 \left[\frac{1}{1-c}\right]^q dx \right\}^n \\ &= \{c^{1-q} + (1-c)^{1-q}\}^n = e^{L(q)n}, \end{aligned} \quad (10)$$

where

$$L(q) = \ln[c^{1-q} + (1-c)^{1-q}]. \quad (11)$$

First of all, notice that for $c = 1/2$, all points of the dynamical system are characterized by the same slope $D_n = 2$. In this case we have:

$$L(q) = \ln \left[\left(\frac{1}{2}\right)^{1-q} + \left(\frac{1}{2}\right)^{1-q} \right] = q \ln 2 \quad . \quad (12)$$

Secondly, for $c > 1/2$ (and in particular for c very close to 1) the system is characterized by two different slopes, $1/c < 2$ and $1/(1-c) > 2$; this means that there are states of the system for which the error growth is ‘slow’ ($x \in [0, c]$) and states for which the error growth is ‘fast’ ($x \in [c, 1]$). In this case, $L(q)$ is no longer characterized by a single time scale.

Coming back to the interpretation of eq. (7) and assuming that $R(t, 0)$ already shows an exponential behavior, we can write:

$$R(t, 0) \sim e^{\gamma t}, \quad (13)$$

where γ is the *local* error growth exponent; the error growth exponent is local in the sense that it depends on the particular initial condition under consideration. We now briefly review how λ_1 can be seen as the average over all possible local exponents of the system. We can rewrite $R(t, 0)$ as:

$$R(t, 0) = \prod_{i=1}^M R(t_i, t_{i-1}), \quad (14)$$

where $0 = t_0 < t_1 < \dots < t_i < t_{i+1} < \dots < t_M = t$, and we are regarding the trajectory as a sequence of M trajectories. By introducing the notation:

$$R(t_i, t_{i-1}) \sim e^{\gamma_i(t_i - t_{i-1})}, \quad (15)$$

we have:

$$e^{\gamma t} = e^{\sum_{i=1}^M \gamma_i(t_i - t_{i-1})}. \quad (16)$$

Therefore, assuming $t_i - t_{i-1} = \Delta t$ for any i , we have $t = M\Delta t$ and

$$\gamma = \frac{1}{M} \sum_{i=1}^M \gamma_i. \quad (17)$$

Equation (17) tells us that γ is just the average value of γ_i ’s along the trajectory. By the Oseledec (1968) theorem we know that, for $t \rightarrow \infty$ (i.e., for $M \rightarrow \infty$), $\gamma \rightarrow \lambda_1$. Thus, λ_1 is the average over all possible local exponents γ_i of the system. We can now ask what is the probability of having $\gamma \neq \lambda_1$ for finite times. In order to answer this question, we introduce the probability $P_t(\gamma)$ of the local error growth being equal to γ at time $t = M\Delta t$. The introduction of a p.d.f. $P_t(\gamma)$ is possible under the ergodicity assumption

(for a review of the ergodic theory, see for example Halmos (1956)). The p.d.f. is then related to the existence of an attractor set, described by an invariant measure, which can be operatively defined by computing the average fraction of the time spent by the evolving system in any portion of the attractor. The quantity $\langle R(t, 0)^q \rangle$ can be expressed by the integral:

$$\langle R(t, 0)^q \rangle = \int P_t(\gamma) e^{\gamma q M \Delta t} d\gamma. \quad (18)$$

As already pointed out, only for $M \rightarrow \infty$ do we have $P_t(\gamma) \rightarrow \delta(\gamma - \lambda_1)$. For finite but large M , the large deviations theory (for a general presentation see Varadhan (1984) and Ellis (1985); for a more physical treatment see Frisch (1995)) characterizes $P_t(\gamma)$ as:

$$P_t(\gamma) \sim e^{-S(\gamma)M\Delta t}, \quad (19)$$

where $S(\gamma)$ is a concave function such that $S(\gamma) \geq 0$ and $S(\gamma) = 0$ for $\gamma = \lambda_1$. The large deviations theory holds, in its simplest form, for independent random variables. Like the law of large numbers and the central limit theorem, the large deviations theory has extensions to random variables with correlations, when these correlations decrease sufficiently fast. These are the conditions under which $P_t(\gamma)$ takes the form (19). In the language of large deviations theory, $S(\gamma)$ is called *Cramer function* or *Cramer entropy* (Mandelbrot 1991). Different systems will have different p.d.f.'s (i.e., different $S(\gamma)$). In the next part of this subsection we will show how the explicit form of the $L(q)$ exponents can be obtained from the Cramer function $S(\gamma)$ of the system. We will also show the general relation between $L(q)$ and λ_1 .

Inserting (19) into (18), by saddle-point integration one obtains:

$$\langle R(t, 0)^q \rangle \sim \int e^{[\gamma q - S(\gamma)]M\Delta t} d\gamma \sim e^{L(q)M\Delta t}, \quad (20)$$

where

$$L(q) = \sup_{\gamma} [q\gamma - S(\gamma)] \quad (21)$$

and $\sup_{\gamma} [f(\gamma)]$ means the smallest upper bound of the function $f(\gamma)$.

Since $S(\gamma)$ is a concave function, the maximum value of the convex function $q\gamma - S(\gamma)$ is unique and attained at the value γ_q at which

$$\frac{d(q\gamma - S(\gamma))}{d\gamma} \Big|_{\gamma=\gamma_q} = 0 \quad \text{or} \quad \frac{dS(\gamma)}{d\gamma} \Big|_{\gamma=\gamma_q} = q. \quad (22)$$

Thus, from (21) one obtains:

$$L(q) = q\gamma_q - S(\gamma_q) \quad (23)$$

and

$$\frac{dL(q)}{dq} = \gamma_q + q\frac{d\gamma_q}{dq} - \frac{dS(\gamma_q)}{dq} = \gamma_q. \quad (24)$$

Since $L(0) = 0$, it follows from (23) that $S(\gamma_0) = 0$. Thus, as an immediate consequence of the general properties of $S(\gamma)$, one obtains $\gamma_0 = \lambda_1$. From (24) the following expression for the maximum Lyapunov exponent can be obtained:

$$\lambda_1 = \left. \frac{dL(q)}{dq} \right|_{q=0}. \quad (25)$$

The quantities γ_q are the characteristic exponents describing the predictability fluctuations of the dynamical system: if $L(q)$ is a linear function of q , they reduce to a single exponent, namely λ_1 (see eq. (24)). If $L(q)$ does not follow the linear relationship $\lambda_1 q$, then the complete set of exponents γ_q is needed to characterize predictability fluctuations. In this case the system is *intermittent*. The functional form of $L(q)$ depends on the system, and specific assumptions on the p.d.f. $P_t(\gamma)$ have to be made in order to perform a quantitative analysis.

2.1.2 The log-normal case

There is no general theory about the shape of the $S(\gamma)$ function, as different systems may have different predictability fluctuations. If correlations are weak enough, central limit arguments can be applied and a Gaussian law for $P_t(\gamma)$ may be assumed (Paladin and Vulpiani 1987). Several numerical studies (see, for example, Benzi *et al.* 1985; Benzi and Carnevale 1989) show to what degree the log-normal hypothesis for the statistics of the error growth can reproduce the computed $L(q)$'s for simple dynamical and atmospheric models. Let us recall here the main points which follow from this hypothesis, assuming a quadratic behavior for $S(\gamma)$:

$$S(\gamma) = (\gamma - \lambda_1)^2/2\mu. \quad (26)$$

From eqs. (19) and (26) it follows that the normalized p.d.f. for γ reads:

$$P_t(\gamma) = \frac{1}{\sqrt{2\pi\mu/t}} e^{-\frac{(\gamma-\lambda_1)^2}{2\mu/t}}. \quad (27)$$

From the transformation rule $P_t(R) = P_t(\gamma(R)) \left| \frac{d\gamma}{dR} \right|$, the log-normal distribution for the response function $R(t, 0)$ follows as:

$$P_t(R) = \frac{1}{R\sqrt{2\pi\mu t}} e^{-\frac{(\ln R - \lambda_1 t)^2}{2\mu t}}. \quad (28)$$

The probability distribution is thus fully characterized by two parameters only:

$$\begin{aligned} \lambda_1 &= \langle \ln R(t, 0) \rangle / t, \\ \mu &= [\langle (\ln R(t, 0))^2 \rangle - \langle \ln R(t, 0) \rangle^2] / t, \end{aligned} \quad (29)$$

where λ_1 is the maximum Lyapunov exponent and μ is the second cumulant.

In the general case, the parameters λ_1 and μ , as defined in (29), continue to be important, although they may not completely represent the p.d.f.: they give respectively the mean value and the variance of the γ -fluctuations. For this reason, the μ parameter is usually referred to as the intermittency of the system. The ratio $\mu/\lambda_1 = 1$ may be taken as the borderline between weak and strong intermittency. About the latter regime, an important point has to be stressed. Consider the most probable response function value \tilde{R} (obtained by solving $\frac{dP_t(R)}{dR} = 0$) and the mean value $\langle R \rangle$. In the log-normal case their expressions read:

$$\tilde{R} = e^{\lambda_1 t(1 - \mu/\lambda_1)} \quad \text{and} \quad \langle R \rangle = e^{\lambda_1 t(1 + \mu/(2\lambda_1))}. \quad (30)$$

From eqs. (30) it follows that a rough estimate of the response that, for example, takes the most probable value \tilde{R} as representative of the distribution, fully breaks down for $\mu/\lambda_1 > 1$. This approximation predicts a decreasing error for long times ($\lim_{t \rightarrow \infty} \tilde{R} = 0$) instead of the chaotic error growth characterized by a positive exponent ($\lim_{t \rightarrow \infty} \langle R \rangle = \infty$).

Using $S(\gamma)$ given by (26) in the expression (22) we obtain:

$$\gamma_q = \lambda_1 + \mu q \quad (31)$$

which, substituted into (23), gives the generalized Lyapunov exponents for the log-normal case:

$$L(q) = \lambda_1 q + \frac{1}{2} \mu q^2. \quad (32)$$

As a reasonable definition of the characteristic predictability time T of the system, one can consider the following, which takes into account the effects of fluctuations:

$$T \sim \frac{1}{L(1)} \sim \frac{1}{\lambda_1 + (1/2)\mu}. \quad (33)$$

It is reasonable to assume that, in the general case, $L(q)$ would be bounded between the linear shape (i.e., absence of fluctuations) and the quadratic shape (i.e., strong fluctuations). In many cases, the log-normal shape is a good approximation for small deviations of γ around its mean value, i.e., it reproduces quite well the smallest moments of the distribution. On the other hand, for large q 's, the moments cannot be of the log-normal type (Paladin and Vulpiani 1987), since log-normal moments grow more than exponentially with q . This implies that $\lim_{q \rightarrow \infty} \gamma_q$ is not finite. This limit is related to the fastest error growth R^* in the system, which must be finite for all physical systems. The log-normal approximation fails to reproduce the tails of the distribution $P_t(R)$, that is, the largest fluctuations.

2.1.3 The log-Poisson case

The physical constraint that the fastest error growth must be finite forces one to look for parametrizations of $P_t(\gamma)$ other than Gaussian. For this purpose, let us introduce, for the first time to our knowledge in predictability theory, recent ideas developed in statistical treatment of fully developed turbulence (the basic concepts can be found in She and Waymire (1995)).

One way to consider alternative probability distributions is by observing that the quantity:

$$R(t', t) = \frac{|\delta \mathbf{x}(t')|}{|\delta \mathbf{x}(t)|} \quad (34)$$

obeys the multiplicative rule:

$$R(t', t) = R(t', t'')R(t'', t), \quad (35)$$

for any t'' . Thus, one is led to consider all possible probability functions $P_t(\gamma)$ which are left functionally invariant by the multiplicative transformation (35). We shall call this class of probability functions covariant.

By making the (strong) assumption of weak correlation between $R(t', t'')$ and $R(t'', t)$, an important class of distributions turns out to be covariant: this is the class of the *infinitely divisible distributions* (IDD). The normal and the Poisson distributions are the most popular examples of IDD (for a comprehensive list and demonstrations of the properties of IDD, see for example Doob (1990)).

In the following we shall consider the Poisson distribution as the simplest example of a non-Gaussian IDD that gives a more suitable description of strong fluctuations than the Gaussian distribution. As we shall see, it permits also to satisfy the physical constraint that the fastest error growth has to be finite.

Notice that this simple (and discrete) stochastic model is not intended to represent the p.d.f. of a generic (continuous) physical system. Our aim here is twofold: on one hand, we show that the Poisson distribution, in spite of its simplicity, shares some important properties with realistic p.d.f.'s; on the other hand, we show that statistical quantities can be successfully fitted by using the Poisson formulation. In this sense, the Poisson assumption gives a simple way to characterize and quantify some predictability properties.

Let us rewrite the response function in terms of a Poisson random variable x , factorizing its exponential time dependence:

$$R(t, 0) \sim e^{at} \beta^x, \quad (36)$$

where $\beta \leq 1$ and x is a random variable that follows the Poisson distribution:

$$P_t(x = n) = \frac{(bt)^n e^{-bt}}{n!}. \quad (37)$$

Using eq. (37), the q th-order moment of the response function R can be easily calculated:

$$\langle R^q \rangle = \sum_n \frac{(bt)^n e^{-bt}}{n!} e^{aqt} \beta^{qn} = e^{(aq-b)t} \sum_n \frac{(bt\beta^q)^n}{n!} = e^{[aq-b(1-\beta^q)]t} \quad (38)$$

and the expression for the generalized Lyapunov exponents becomes:

$$L(q) = aq - b(1 - \beta^q). \quad (39)$$

From eqs. (24) and (25) we also obtain

$$\gamma_q = a + b\beta^q \ln \beta \quad \text{and} \quad \lambda_1 = a + b \ln \beta. \quad (40)$$

Notice that for large q 's the generalized Lyapunov exponents given by (39) behave as $L(q) \sim aq - b$. The a parameter is associated with the fastest error growth in the system, $R^* = e^{at}$, which is finite. Thus, the log-Poisson p.d.f. does not show the pathologies typical of the log-normal distribution.

A comparison between R^* and $\langle R \rangle$ can give a measure of intermittency, namely:

$$\frac{\ln R^*}{\ln \langle R \rangle} = \frac{a}{L(1)} \equiv \tilde{a}. \quad (41)$$

To summarize, the considerations outlined in this section allow us to investigate predictability properties at large t (i.e., on the attractor set) by means of quantities such as λ_1 , μ and $L(q)$. In particular, one can consider the ratio μ/λ_1 (particularly important if a log-normal hypothesis is made) or the ratio \tilde{a} (in the case of log-Poisson statistics) as measures of predictability fluctuations.

2.2 Characterization of predictability fluctuations at short times

In this section we show, with the help of a simple example, how it is possible to extract quantitative information about the predictability fluctuations of a system in the super-exponential error growth regime. Here and for the first time in a meteorological context, we use recent techniques employed in turbulence data analysis, which lead to a generalization of the concepts previously reported for the asymptotic regime. Again, the simple Poisson assumption can be made and useful statistical quantities can be evaluated.

We are here concerned with the response function for a finite time interval. A statement about the choice of initial conditions has thus to be made. In the following, we make the familiar assumption of an homogeneous and isotropic probability distribution of the disturbance vector in phase space, which was assumed originally by Lorenz (1965).

2.2.1 An example

In order to discuss the predictability fluctuations at short times, we will consider the Lorenz (1963) system (hereafter L63). For $r \sim 24.74$ (the critical value for the fixed points to be unstable) a linear behavior of $L(q)$ is found (see Benzi *et al.* 1985): the system does not show intermittency in the long times regime. The same behavior does not hold for short times, which are relevant in meteorological applications.

This point can be detected in Fig. 2, where the second and sixth order moments of the response function R are shown, as an example, as a function of time for $r = 28$. In both graphs, two temporal ranges are clearly detectable (the noise in the signal is simply due to lack in statistics). For $t \gtrsim \tau = 1.25$ there is evidence of an exponential error growth, whose exponent, in these log-linear plots, is given by the slope of the straight line fitting the data: the slopes are $L(2) \sim 2\lambda_1 \sim 1.6$ (see Fig. 2(a)) and $L(6) \sim 6\lambda_1 = 4.8$ (see Fig. 2(b)). These values confirm the linear law $L(q) = q\lambda_1$ for the generalized Lyapunov exponents found by Benzi *et al.* (1985).

At shorter times ($t \lesssim \tau$), the error grows more rapidly. Furthermore, a zoom over $t \lesssim 0.2$ reveals a non-exponential behavior of the response function. This feature makes it difficult to extract informations from the data inside the range $0 \leq t \lesssim \tau$.

Notice that the separation between the two temporal regimes takes place at a time scale τ which can be identified to be $\tau \sim 1/\lambda_1$. This seems to be a non-trivial result, even if more examples based on other models are necessary to get the confidence that this property is general and not merely a coincidence.

In order to determine the statistical properties of the error growth at small t , we try to consider different representations of our data. Let us consider, as an example, the log-log plot of the sixth order moment against the second order moment (Fig. 3). As one can see, such representation reduces the spreading of points with respect to Fig. 2, thus improving the quality of the linear fit. Furthermore, a zoom corresponding to the temporal range $t \lesssim 0.2$ (inside box in Fig. 3) reveals the following key point: a linear behavior now takes place from very early time and a measure of intermittency now

becomes possible. The best fit for long times ($t1/\lambda_1$) gives the ratio $L(6)/L(2) \sim 3$ (i.e., no intermittency is present in the long-time regime). For $t < 1/\lambda_1$ this ratio gives the values 4.9, indicating a nonlinear behavior of $L(q)$ and thus the intermittent nature of the system for short times.

Fig. 3 represents one of the main results obtained in this paper.

From this example we argue that it is possible to achieve a quantitative measure of predictability fluctuations even at short time, when non-exponential growth rates are observed.

2.2.2 The ESS analysis at short times

The results of Fig. 3 suggest to try a generalization of the concepts reported in sec. 2.1. Accordingly, one can continue to assume the covariance property (35) to be valid even for a time-dependence of the response $R(t, 0)$ different from the exponential one.

Thus, the hypothesis of IDD's governing the error growth statistics continue to hold in the transient regime. As an example, let us consider again the Poisson case. The temporal dependence e^t may be replaced by a more general function $g(t)$, such that $g(0) = 1$ and $\lim_{t \rightarrow \infty} g(t) = e^t$. Relation (36) becomes:

$$R(t, 0) \sim g(t)^a \beta^x, \quad (42)$$

where x is a random variable with a Poisson distribution:

$$P_t(x = n) = \frac{[b \ln g(t)]^n e^{-b \ln g(t)}}{n!}. \quad (43)$$

From (42) and (43), it follows that the statistical moments of the response function at short t take the form:

$$\langle R(t, 0)^q \rangle \sim e^{L(q) \ln g(t)}, \quad (44)$$

with $L(q)$ given by (39).

The results of Fig. 3 suggest that one may extract information about predictability fluctuations in the system by considering ratios like $\ln \langle R^q \rangle / \ln \langle R^p \rangle$, which allow us to eliminate the functional dependence on $g(t)$. This is the basic idea of the *Extended Self Similarity* (ESS) techniques recently employed in fully developed turbulence (Benzi *et al.* 1993; Benzi *et al.* 1995): they concern the possibility of observing a scaling behavior of turbulent velocity and energy dissipation fields over an enlarged range of spatial scales and in systems and conditions where these scaling properties are not evident with standard techniques.

The above simple considerations allow extending the notion of generalized Lyapunov exponents in a simple way. Accordingly, we can define the quantities:

$$\frac{\ln\langle R^q \rangle}{\ln\langle R \rangle} = \frac{L(q) \ln g(t)}{L(1) \ln g(t)} \equiv \tilde{L}(q). \quad (45)$$

The constraint $\tilde{L}(1) = 1$ leaves only two free parameters, $\tilde{a} = a/L(1)$ and $\tilde{b} = b/L(1)$. As already noted (see Eq. (41)), the quantity \tilde{a} has a straightforward meaning and can be considered as a useful intermittency indicator.

By measuring $\tilde{L}(q)$ exponents, it is thus possible to obtain quantitative information about predictability properties even at short times.

Let us conclude this section by introducing another new indicator that we consider useful in studying

predictability fluctuations at short times. We define the quantity $\tilde{P}(t)$ as:

$$\tilde{P}(t) = \int_{R \leq 1} P_t(R) dR, \quad (46)$$

where $P_t(R)$ is the p.d.f. of the response function $R(t, 0)$.

The quantity $\tilde{P}(t)$ is the probability of observing an error $\delta\mathbf{x}(t)$ smaller or equal to the initial error $\delta\mathbf{x}(0)$. By construction, we have $\tilde{P}(0) = 1$, while in the limit of large t , $\tilde{P}(t) \rightarrow 0$. If there are no fluctuations in the predictability exponents, one obtains $\tilde{P}(t) = 0$ for every $t \neq 0$. This is not the case for intermittent systems.

Let us compare the cases of log-normal and log-Poisson distributions. For a log-normal distribution, $\tilde{P}(t)$ decreases monotonically toward zero. An easy way to see it is the following: after substituting eq.(28) into eq.(46) and defining the variable

$$z = \frac{\ln R - \lambda_1 t}{\sqrt{2\mu t}}, \quad (47)$$

one obtains the following expression of eq.(46) for the log-normal case:

$$\tilde{P}(t) = \int_{-\infty}^{-\frac{\lambda_1}{\sqrt{2\mu}}\sqrt{t}} \frac{e^{-z^2}}{\sqrt{\pi}} dz. \quad (48)$$

The dependence on t is now only in the upper bound of the integral: as time increases, the range of integration decreases, thus making $\tilde{P}(t)$ a monotonically decreasing function of t .

On the other hand, the short-time behavior in the log-Poisson case is completely different: $\tilde{P}(t)$ grows as $(1 - e^{b \ln g(t)})$, up to a time \bar{t} such that $g(\bar{t}) = \beta^{-1/a}$. Then, for large t , it decays toward zero, following a typical step behavior induced by the discrete character of the Poisson distribution.

The above considerations imply that in an intermittent system the probability of observing an error smaller or equal to the initial error can be finite. Moreover, the behavior of $\tilde{P}(t)$ for small t is completely different in the two cases of log-Poisson and log-normal distributions. This effect is due to the finite maximum growth rate of the Poisson case: the finiteness of the parameter a allows a growth of $\tilde{P}(t)$ for $t \leq \bar{t}$.

These considerations illustrate the straightforward physical meaning of the quantity $\tilde{P}(t)$ in predictability studies concerning the short time range. Moreover, a systematic, quantitative investigation may be performed at any time by evaluating the $\tilde{L}(q)$ exponents.

3 Application to a low-order primitive equation model

In order to apply the theory outlined in the previous section, we have considered the low-order model for atmospheric flow introduced by Lorenz (1980). This model represents a suitable truncation of simplified primitive equations (hereafter PE) on β -channel. As in Lorenz (1980), the model equations are:

$$a_i \frac{dx_i}{d\tau} = a_i b_i x_j x_k - c(a_i - a_k) x_j y_k + c(a_i - a_j) y_j x_k - 2c^2 y_j y_k - \nu_0 a_i^2 x_i + a_i (y_i - z_i) \quad (49)$$

$$a_i \frac{dy_i}{d\tau} = -a_k b_k x_j y_k - a_j b_j y_j x_k + c(a_k - a_j) y_j y_k - a_i x_i - \nu_0 a_i^2 y_i \quad (50)$$

$$\frac{dz_i}{d\tau} = -b_k x_j (z_k - h_k) - b_j (z_j - h_j) x_k + c y_j (z_k - h_k) - c(z_j - h_j) y_k + g_0 a_i x_i - \kappa_0 a_i z_i + F_i \quad (51)$$

where x_i , y_i and z_i are the coefficients of the velocity potential, streamfunction and height fields, respectively. Here, (i, j, k) stands for any permutation over $(1, 2, 3)$. For our studies, we have used physical parameter values which correspond to large scale motion in the mid-latitude atmosphere, in agreement with previous works (Lorenz 1980; Gent and McWilliams 1982; Vautard and Legras 1986; Lorenz 1986; Curry *et al.* 1995)

The evolution equations for an infinitesimal error have been obtained by linearization of eqs. (49-51). For all simulations presented in this paper, the familiar assumption of homogeneous and isotropic p.d.f. of the initial disturbance vector in the phase space is made (Lorenz 1965). The number of realizations (i.e., different trajectories) considered is of the order of 10^4 . For each realization of the ensemble, the initial error has been randomly selected on the sphere centered at the initial point of the trajectory. The numerical integrations have been performed using a fourth-order Runge-Kutta scheme.

In order to show the capability of the parameter μ/λ_1 to capture the fluctuations in the predictability, let us consider the three different regimes of the PE model discussed by

Krishnamurthy (1985), corresponding to three different values of the forcing parameter: $F_1 = 0.1$, $F_1 = 0.25$ and $F_1 = 0.3$. The physical regimes associated with such values are the following (for details, see Krishnamurthy (1985)): for $F_1 = 0.1$ the attractor of the PE system is free from gravity waves; for $F_1 = 0.25$ the trajectories vary chaotically, with an almost periodic behavior interrupted irregularly by short periods characterized by high frequency gravity waves; finally, for $F_1 = 0.3$, gravity waves are present all the time.

To evaluate the two parameters λ_1 and μ , defined in (29), each realization (trajectory) has been made to last for a time t of the order of a hundred days, large enough to apply all the considerations of sec. 2.1.

In Tab. 1, the values of the positive maximum Lyapunov exponent, the intermittency, the ratio μ/λ_1 , and the predictability time T for the PE system in the three aforementioned regimes are shown. As already noted, the value of $\mu/\lambda_1 = 1$ could be considered as the borderline between weak and strong intermittency. We can see from Tab. 1 that three different values of μ/λ_1 occur in the three regimes. The signature of the gravity wave activity, in the cases $F_1 = 0.25$ and $F_1 = 0.3$, is emphasized by the enhancement of both λ_1 and μ , with respect to the case $F_1 = 0.1$. The predictability of the system is thus reduced by persistent gravity waves. It is also worth noticing that strong intermittency (i.e., $\mu/\lambda_1 > 1$) is present only in the intermediate case $F_1 = 0.25$, characterized by the appearance of bursts of chaoticity containing high frequency gravity waves.

For the regime $F_1 = 0.1$, we have also performed a systematic numerical investigation of the generalized Lyapunov exponents at long and short times. The logarithm of the sixth order moment of the response function R as a function of time is reported in Fig. 4. Two regions are clearly detectable. For t large enough ($t \gtrsim 1/\lambda_1 \sim 16 \text{ days}$) the points can be fitted by a straight line, indicating an exponential error growth: the slope of the fitting line gives the sixth order generalized Lyapunov exponent $L(6)$ (the noise in the signal is simply due to lack in statistics). At shorter times ($t \lesssim 1/\lambda_1$), the error grows more rapidly; moreover, a zoom over the first 5 days reveals a strongly nonlinear behavior. As we shall see in the next section, this is mainly associated with the presence of transient gravity waves, whose amplitude is significant, especially in very the first times of integration.

Notice that, as in the L63 model, the characteristic time scale associated with a change in the error growth regime is of the order of $1/\lambda_1$.

The use of ESS techniques allows us to improve the quality of the fit in the long-time region and to extract information on generalized Lyapunov exponents even at small t . As an example, the sixth order moment against the first order moment is shown in Fig. 5 in a log-log plot. We can see from the zoom over the 5 day temporal range that a linear behavior occurs from very early times. We have then evaluated for 14 moments ($q=0.2, 0.4, 0.6, 0.8, 1, 2, \dots, 10$) the $\tilde{L}(q)$ exponents at short and long times, by performing linear fits in the two temporal regions $0 < t \leq 10$ days and $40 \leq t \leq 300$ days, respectively. The results are shown in Fig. 6 : the points are well fitted by the

log-Poisson formula, with parameters $\tilde{a}_l = 1.2$, $\tilde{b}_l = 0.3$ (for the long-time $\tilde{L}(q)$ values) and $\tilde{a}_s = 4.5$, $\tilde{b}_s = 4.3$ (for the short-time $\tilde{L}(q)$ values). In particular, notice that $\tilde{a}_s > \tilde{a}_l$, as the comparison of the two slopes at high q 's shows. This is a quantitative indication of the more intermittent nature of the system for short times (see eq. (41)).

Focusing our attention on the short-time regime, we have also evaluated the function $\tilde{P}(t)$ defined in sec. 2.2, by counting the number of realizations (trajectories) having $R(t, 0) < 1$ at a certain time t :

$$\tilde{P}(t) = \frac{N_{R(t,0) < 1}}{N_{tot}}. \quad (52)$$

Fig. 7 shows the $\tilde{P}(t)$ for the PE model. Due to the appearance of transient gravity waves, a very strong loss of predictability occurs immediately after the beginning of the PE model integration: $\tilde{P}(t)$ is close to 0 and starts to grow until $\bar{t} \sim 5$ days, a behavior in qualitative agreement with a log-Poisson character of the $R(t, 0)$ p.d.f.. After about 10 days, gravity waves become lost and only slow oscillations remain.

From the above results, it appears that the presence of gravity waves (on the attractor set as well as in the initial transient) has strong effects on predictability. In particular, the loss of predictability immediately after the first times of the model integration may be relevant for practical purposes. The final question we want to address is thus the following: may the elimination of gravity waves produce an enhanced short-time predictability? We shall try to answer this question in the next section.

4 Predictability fluctuations and their relations with gravity wave activity

Our first aim is to study how the predictability fluctuations are influenced by the disappearance of gravity waves in models not supporting such waves.

We shall focus our attention on Lorenz's (1980) algorithm exploiting the complete separation between quasi-geostrophic and gravity wave frequencies, and leading to the well-known superbalance equation, defining the *slow manifold* (Leith 1980; Lorenz 1980).

Defining $\mathbf{X}^G = (X_1^G, X_2^G, X_3^G, X_4^G, X_5^G, X_6^G)$, where $X_i^G = x_i$ and $X_{i+3}^G = z_i - y_i$ for $i = 1, 2, 3$, while $\mathbf{X}^R = (y_1, y_2, y_3)$, Lorenz (1980) exploited the scale separation imposing the condition $\frac{d^p \mathbf{X}_{p,k}^G}{dt^p} = 0$ which can be solved iteratively for each p by the Newton method (Lorenz 1980).

The low-order dynamical system obtained from the PE model by calculating the \mathbf{X}^G components through Lorenz's algorithm (with $p = 1$) is called here *SuperBalance Equation* (SBE) model.

We apply the notions outlined in sec. 2.1 and 2.2 to the PE and SBE models in order to quantify the effects of gravity wave activity on the predictability fluctuations.

The positive maximum Lyapunov exponent, the intermittency, the ratio μ/λ_1 and predictability time T (see eq. (33)) are shown in Tab. 2 for the two models. Actually, as we can see from this table, these asymptotic quantities do not permit us to discriminate between the PE and SBE models. The very slight differences in these chaotic indicators confirm the capability of SBE to reproduce the asymptotic statistical properties of the PE system. Let us then come back to the original question: in what sense does elimination of transient gravity waves make the SBE model less chaotic than the PE model?

An answer to this question can be given by exploiting the short-time analysis presented in sec. 2.2. In Fig. 8 we report the same plot of Fig. 4, but for the SBE model. As in the PE model, two regions are clearly detectable, with the error growth for short times faster than that for long times. However, the zoom over the first 5 days shows an exponential (that is linear in the graph) error growth since the very first time, unlike the PE case. This is due to the projection onto the slow manifold which causes the gravity waves to die out completely.

In order to improve the quality of the fit and make a comparison possible, we perform for the moments of the error growth the same ESS analysis already presented for the PE case. In particular, $\tilde{L}(q)$ exponents of the SBE model in the long-time regime turn out to be indistinguishable from those of the PE model shown in Fig. 6 (white circles). This fact confirms the success of the SBE model in reproducing the asymptotic statistical properties of the Lorenz model.

Let us focus our attention on the short-time behavior. The $\tilde{L}(q)$ exponents for the SBE model, obtained from a linear fit at short time, are reported in Fig. 9. In order to simplify the comparison, the corresponding curve for the PE model (already reported in Fig. 6 (black circles)) is shown. Several comments are worthwhile. The log-Poisson fit for the SBE model gives $\tilde{a}_s = 2.9$ and $\tilde{b}_s = 2.4$: in particular, we stress that the slopes \tilde{a}_s are smaller than in the PE case. Hence, disappearance of gravity waves in the SBE model decreases temporal intermittency, damping predictability fluctuations in a sensible way.

The enhanced predictability during the first days becomes more evident if one considers $\tilde{P}(t)$ behavior for the PE and SBE models, shown in Fig. 10. As we can see, the SBE curve strongly differs from that of the PE system during the first days. Notice that the $\tilde{P}(t)$ starts near 1 for the SBE model. It then follows that the very strong loss of predictability (i.e., $\tilde{P}(t)$ close to 0) immediately after the first times of the PE model integration is certainly due to the transient gravity waves: for the SBE model, where gravity waves are not present, there is only a slight loss of predictability (i.e., $\tilde{P}(t)$ close to 1) during the first few days.

After about 10 days, gravity waves disappear in the PE system and the behavior of $\tilde{P}(t)$ for the two models becomes quite similar. From the behavior of both $\tilde{L}(q)$ and $\tilde{P}(t)$, we can conclude that the SBE model systematically produces at short times a more predictable flow with respect to the PE model. To our knowledge, this is the first statistical assessment concerning the effects introduced

by initialization procedures on the predictability properties of an atmospheric model.

5 Conclusions

In the Introduction we have posed three different questions which we believe are relevant for the predictability problem in atmospheric flows.

The answer to the first question we posed (how to describe predictability fluctuations) can be given in terms of generalized Lyapunov exponents, $L(q)$'s, which represent the growth rate of the moments of the response to an initial error. The statistics of $R(t, 0)$ are characterized by an infinite set of exponents related to $\langle R(t, 0)^q \rangle$. The non linearity of $L(q)$ vs q reflects the intermittent nature of the temporal evolution of the error growth. In this sense, this infinite set of exponents contains a level of information which is not present in the maximum Lyapunov exponent λ_1 , λ_1 being able to quantify only the average predictability properties of a system. The use of $L(q)$'s is not completely new. They have been already introduced in the framework of atmospheric models by Benzi and Carnevale (1989). Regarding specific hypothesis on the $R(t, 0)$ p.d.f., they considered the log-normal case. Here we have proposed the use of a log-Poisson p.d.f. (recently introduced in the statistical theory of turbulence for the treatment of spatial intermittency, see for example She and Waymire (1995)) to overcome some of the deficiencies of the log-normal p.d.f..

We have also focused our attention on the short-time predictability properties which is a rather complex problem. The fact that the error growth need not be exponential for short times makes the analysis more difficult, introducing a complex functional dependence of the response function on the time t , which can vary depending on the system.

Using recent ideas introduced and applied in the context of fully developed turbulence, namely the Extended Self Similarity techniques, we have shown that the concepts of the generalized Lyapunov exponents can be extended to the short-time regime, introducing the $\tilde{L}(q)$ exponents. They are well-defined mathematical quantities that allow us to quantify the intermittency in the system also at short times. This is one of the major results achieved in this paper.

As a further measure of predictability fluctuations at short time, we have also considered the probability to have a decrease of the initial error at time t (what we called $\tilde{P}(t)$): this is a clear indicator concerning the possibility to have convergence of two trajectories at finite time, due to large fluctuations around the average error growth.

We have applied these concepts to the case of a simple atmospheric model (Lorenz, 1980), which captures some features of synoptic scale motions at mid-latitudes. We chose this model because its numerical study does not need the computational resources necessary in the case of more complex and realistic models. Moreover, in spite of its simplicity, the model has a rich dynamics, characterized by appearance of the so-called

gravity wave modes. This property has allowed us to answer the third question posed in the Introduction, that is, which is the connection, if any, between short-time predictability fluctuations and initialization procedures. To this end, we have considered the initialization procedure proposed by Lorenz (1980) leading to the SBE model.

Our results concerning the PE and SBE models can be summarized as follows:

- the generalized Lyapunov exponents evaluated for the PE and SBE models are well-reproduced by a statistical law of the log-Poisson type and differ both from the non-intermittent linear law $L(q) \propto q$ and the quadratic form implied by a log-normal assumption;
- we have observed in the models two different regimes, associated with two temporal ranges: in the short-time regime, the error grows more rapidly and intermittently than in the asymptotic region. This means that standard (asymptotic) chaotic indicators as λ_1 and μ can be meaningless when considering short-time regimes;
- comparing the asymptotic behaviors of the models, we conclude that the SBE procedure is successful in reproducing the long-time statistics of the original PE model, since all the asymptotic chaotic indicators are practically indistinguishable in the two cases;
- elimination of gravity waves in the SBE model strongly influences predictability for short times, giving a more predictable and less intermittent flow. The initialization procedure is then successful in decreasing the intermittency in the short time region, which is strongly influenced by transient fast oscillations in the PE model;
- strongly non-exponential error growth was observed in the case of the model supporting gravity waves (PE) after the first times of the model integrations. This is the signature of the strong gravity wave activity. Non-exponential behavior is strongly reduced in the SBE model, which does not support gravity waves.

We would like to conclude with some remarks and suggestions for future work. It is necessary to better understand the physical meaning both of the transition observed in the predictability properties (short-time and long-time regimes) and the characteristic time at which this transition occurs. This characteristic time seems to be strongly related to the maximum Lyapunov exponent. We think that this feature (which we are currently investigating) is not peculiar only to the models studied in this paper.

Another point regards the study of the growth of non-infinitesimal errors: indeed, in this paper we have considered the error growth in the so-called tangent space, that is, we have studied the behavior of an infinitesimal initial error, governed by the linearized version of the dynamical equations. It would be interesting to perform a similar analysis for finite initial errors, in order to obtain more realistic information on the predictability when the error in the initial conditions cannot be considered infinitesimal.

Finally, we conclude with two remarks concerning the feasibility of our analysis when more complex models involving a large number of variables are considered. First, in our analysis we computed the moments of the response function up to the tenth order just to highlight the effect of predictability fluctuations. Actually, these can be captured also restricting the analysis to lower order moments, thus reducing the related computational effort. Second, since the predictability is characterized by fluctuations, the need for a good statistical ensemble of simulation runs is always crucial. This is independent of the method used to perform the statistical analysis and, in particular, is not peculiar to our method. The reason for this is that for systems characterized by strong intermittency, large fluctuations may occur with a non-vanishing probability and their effects on the predictability have to be properly accounted for in a statistical way. A large amount of statistics has thus to be gathered just in order to sample the tails of the p.d.f., where the rare events are placed. From this point of view, it is clear that over-simplified atmospheric models suggest a possible strategy to tackle the problem of predictability fluctuations.

Acknowledgements

We are grateful to L. Biferale, R. Festa, C.F. Ratto, O. Reale, M. Vergassola and A. Vulpiani for illuminating discussions, and Dr. Claudio Paniconi for reviewing the text. We thank the “Meteo-Hydrological Center of Liguria Region” where part of the numerical analysis was done. The author (2) acknowledge support from the Sardinian Regional Authorities.

References

- Benettin, G., L. Galgani, A. Giorgilli and J. M. Strelcyn, 1980: Lyapunov characteristic exponents for smooth dynamical systems; A method for computing all of them. Part I: Theory, and Part II: Numerical Application. *Meccanica* **15**, 9–20 and 21–30.
- Benzi, R., G. Paladin, G. Parisi and A. Vulpiani, 1985: Characterisation of intermittency in chaotic systems. *J. Phys. A*, **18**, 2157–2165.
- Benzi, R., and G. Carnevale, 1989: A possible Measure of Local Predictability. *J. Atmos. Sci.*, **46**, 3595–3598.
- Benzi, R., S. Ciliberto, R. Tripiccone, C. Baudet, C. Massaioli, and S. Succi, 1993: Extended self-similarity in turbulent flows. *Phys. Rev. E*, **48**, R29–R32.
- Benzi, R., S. Ciliberto, C. Baudet, and G. R. Chavarria, 1995: On the scaling of three-dimensionale homogeneous and isotropic turbulence. *Physica D*, **80**, 385–398.
- Curry, J.H., S. E. Haupt, and M. N. Limber, 1995: Low-order models, initialization and slow manifold. *Tellus*, **47A**, 145–161.
- Doob, J.L., 1990: *Stochastic Processes*. J. Wiley and Sons, 654 pp.
- Eckmann, J.P., and I. Procaccia, 1986: Fluctuations of dynamical scaling indices in nonlinear systems. *Phys. Rev. A*, **34**, 659–661.
- ECMWF, 1992: New developments in predictability. Workshop Proceedings, 13-15 November 1991.
- Ellis, R.S., 1985: *Entropy, Large Deviations and Statistical Mechanics*. Springer, 364 pp.
- Farrell, B. 1985: Transient growth of damped baroclinic waves. *J. Atmos. Sci.*, **42**, 2718-2727.
- Frisch, U., 1995: *Turbulence*, Cambridge Univ. Press, 296 pp.
- Fujisaka, H., 1983: Statistical dynamics generated by fluctuations of local Lyapunov exponents. *Progr. Theor. Phys.*, **70**, 1264–1275.
- Gent, P.R., and J. C. McWilliams, 1982: Intermediate Model Solutions to the Lorenz

- Equations: Strange Attractors and Other Phenomena. *J. Atmos. Sci.*, **39**, 3–13.
- Halmos, P.R., 1956: *Lectures on Ergodic Theory*, Chelsea, 302 pp.
- Krishnamurthy, V., 1985: The slow–manifold and the persisting gravity waves. PHD Thesis, MIT, 146 pp.
- Lacarra, J. and O. Talagrand, 1988: Short range evolution of small perturbations in a barotropic model. *Tellus*, **40A**, 81–95.
- Leith, C.E., 1980: Nonlinear Normal Mode Initialization and Quasi–Geostrophic Theory. *J. Atmos. Sci.*, **37**, 958–968.
- Lorenz, E.N., 1963: Deterministic non–periodic flow. *J. Atmos. Sci.*, **20**, 130–141.
- Lorenz, E.N., 1965: A study of the predictability of a 28-variable atmospheric model. *Tellus* **17**, 321–333.
- Lorenz, E.N., 1980: Attractor sets and Quasi–Geostrophic Equilibrium. *J. Atmos. Sci.*, **37**, 1685–1699.
- Lorenz, E.N., 1986: On the existence of a slow manifold. *J. Atmos. Sci.*, **43**, 1547–1557.
- Mandelbrot, B., 1991: Random multifractals: negative dimensions and the resulting limitations of the thermodynamic formalism. *Proc. R. Soc. Lond., A* **434**, 79–88.
- Molteni, F., R. Buizza, T.N. Palmer, and T. Petroligis, 1996: The ECMWF Ensemble Prediction System: Methodology and validation. *Q.J.R. Meteor. Soc.*, **122**, 73–119.
- Mukougawa, H., M. Kimoto, and S. Yoden, 1991: A relationship between local error growth and quasi–geostrophic states: case study in the Lorenz system. *J. Atmos. Sci.*, **48**, 1231–1237.
- Mureau, R., F. Molteni, and T.N. Palmer, 1993: Ensemble prediction using dynamically conditioned perturbations. *Q.J.R. Meteor. Soc.*, **119**, 299–323.
- Nicolis, C., 1992: Probabilistic aspects of error growth in atmospheric dynamics. *Quart. J. Roy. Meteor. Soc.*, **118**, 553–568.
- Oseledec, V.I., 1968: A multiplicative ergodic theorem. Lyapunov characteristic

numbers for dynamical systems. *Trans. Moscow Math. Soc.*, **19**, 197–231.

Paladin, G., L. Peliti and A. Vulpiani, 1986: Intermittency as multifractality in history space. *J. Phys. A*, **19**, L991–L996.

Paladin, G., and A. Vulpiani, 1987: Anomalous scaling laws in multifractal object. *Phys. Rep.*, **156**, 147–225.

Palmer, T.N., R. Mureau and F. Molteni, 1990: The Montecarlo forecast. *Weather*, **45**, 198–207.

She, Z.S., and E. C. Waymire, 1995: Quantized energy cascade and log–Poisson statistics in fully developed turbulence. *Phys. Rev. Lett.*, **74**, 262–265.

Trevisan A., 1993: Impact of transient error growth on global average predictability measures. *J. Atmos. Sci.*, **50**, 1016–1028.

Trevisan A., and R. Legnani, 1995: Transient error growth and local predictability: a study in the Lorenz system. *Tellus*, **47A**, 103–117.

Varadhan, S.R.S., 1984: *An Introduction to the Theory of Large Deviations*. Springer–Verlag, 196 pp.

Vautard, R., and B. Legras, 1986: Invariant Manifold, Quasi–Geostrophy and Initialization. *J. Atmos. Sci.*, **43**, 565–584.

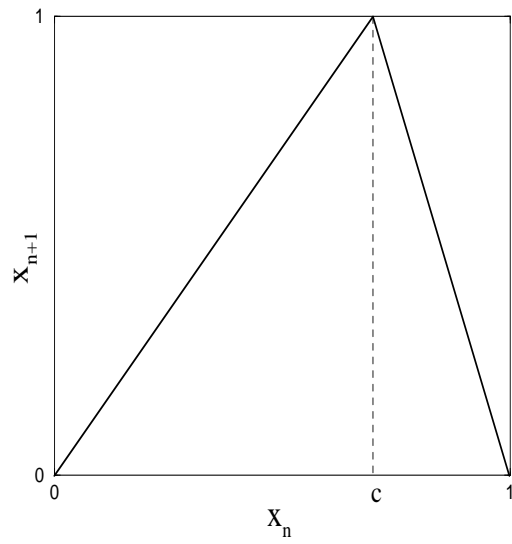


Figure 1: The one-dimensional “tent map”.

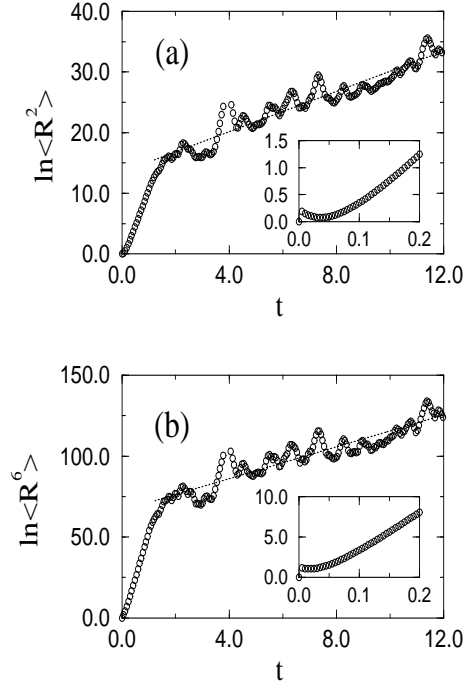


Figure 2: The logarithms of the second (a) and sixth (b) order moments of the response function $R(t, 0)$ as functions of time t for the L63 model. Dotted lines result from linear fits of the data for $t > 1/\lambda_1$: their slopes are $\sim 2\lambda_1$ and $\sim 6\lambda_1$, respectively. Inside boxes are zooms over the very short-time behaviors.

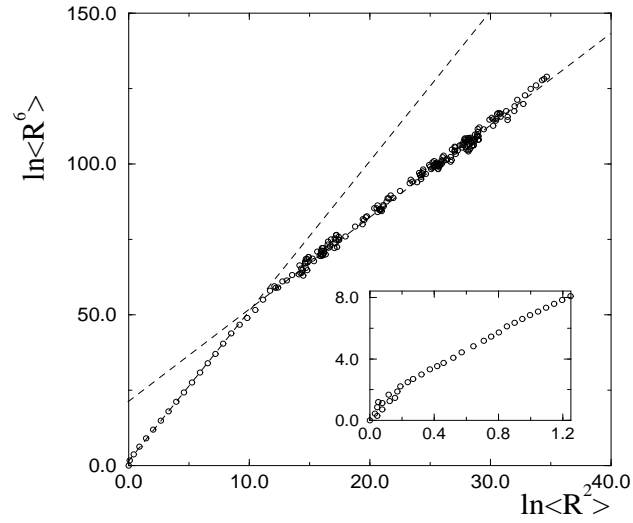


Figure 3: Log-log plot of the sixth order moment against the second order moment of the response function $R(t, 0)$ for the L63 model. Dashed lines result from linear fits of the data in the short and long time regimes. Inside box is a zoom over the very short-time behavior.

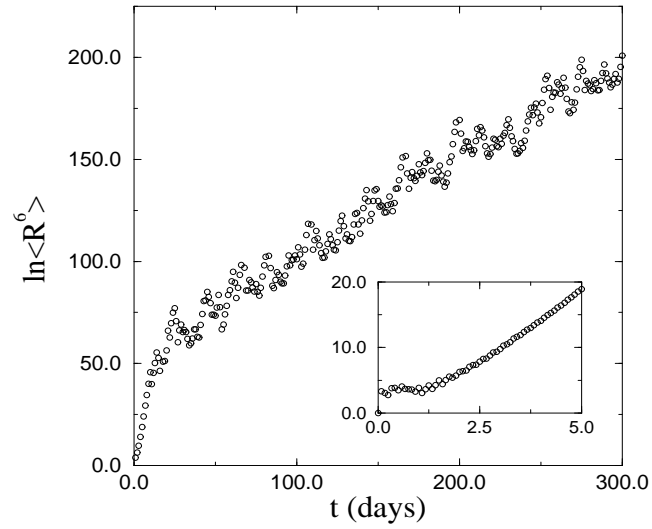


Figure 4: The logarithm of the sixth order moment of the response function $R(t, 0)$ as a function of time t for the PE model. Inside box is a zoom on the first 5 days behavior.

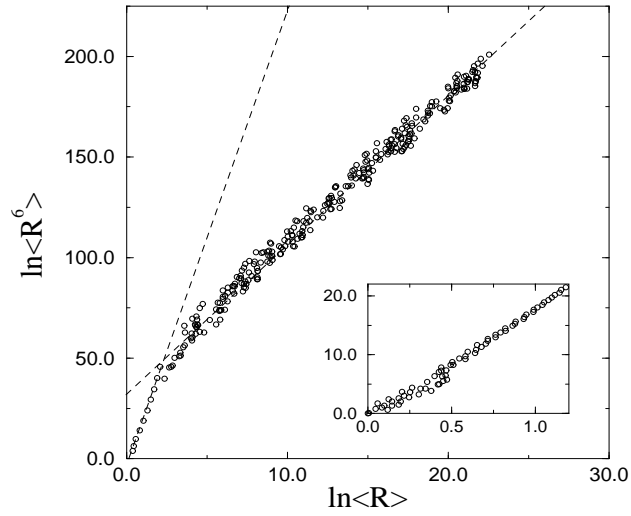


Figure 5: Log-log plot of the sixth order moment against the first order moment of the response function $R(t,0)$ for the PE model. Dashed lines result from linear fits of the data in the short and long time regimes. Inside box is a zoom on the first 5 days behavior.

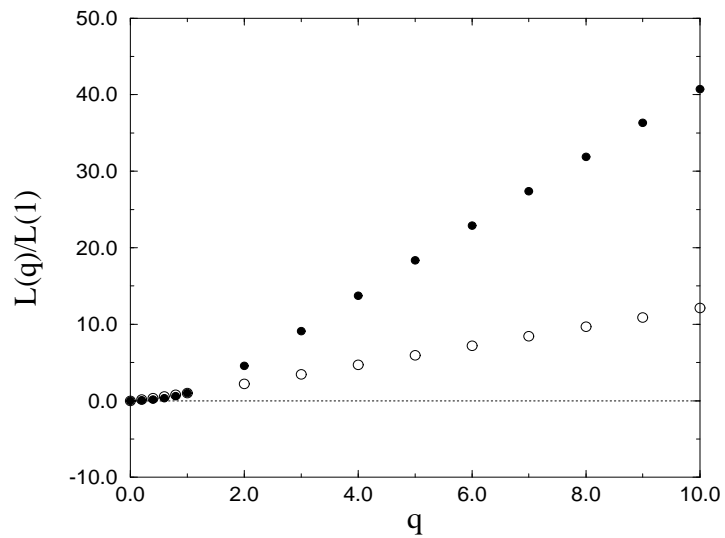


Figure 6: The $\tilde{L}(q)$ exponents as a function of q for the PE model: black circles are the values for $0 < t \leq 10$ days, while white circles denote the long-time values ($40 \leq t \leq 300$ days).

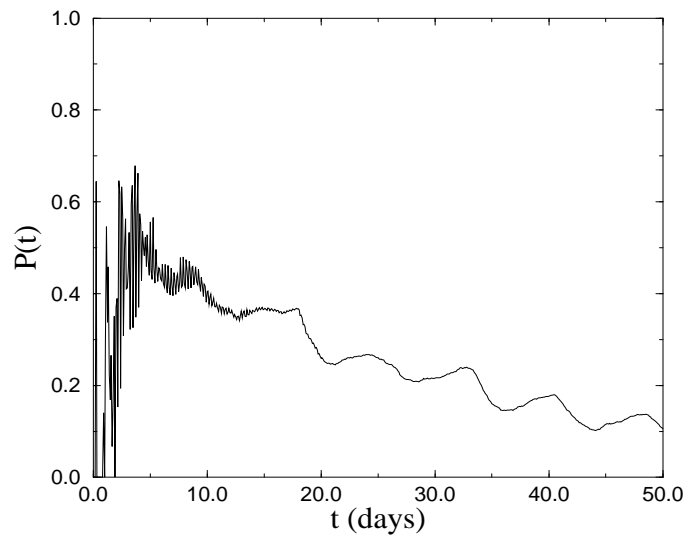


Figure 7: Time behavior of $\tilde{P}(t)$ for the PE model.

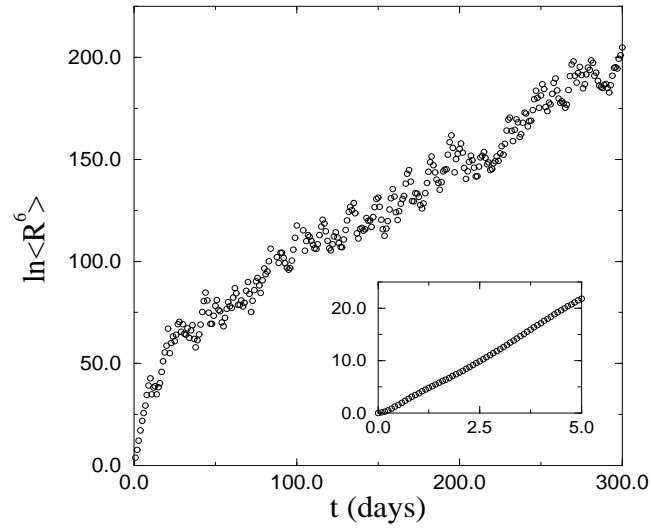


Figure 8: The same as in Fig. 4, but for the SBE model.

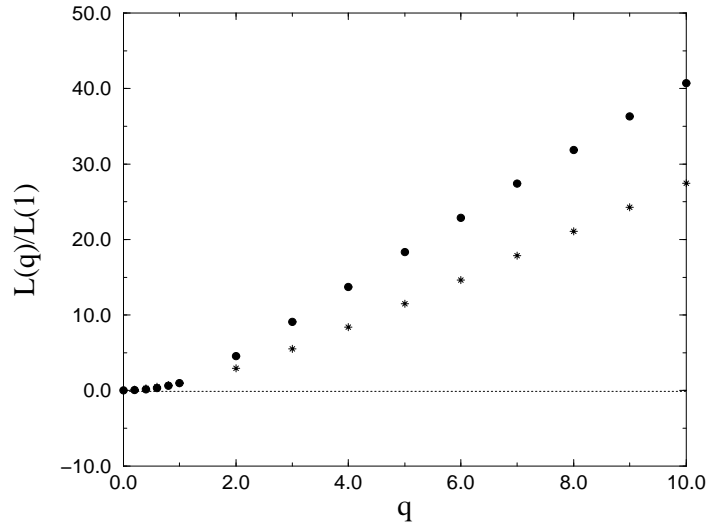


Figure 9: The $\tilde{L}(q)$ exponents as a function of q for the PE and SBE models in the short-time regime ($0 < t \leq 10$ days): circles and stars are the PE and SBE values, respectively.

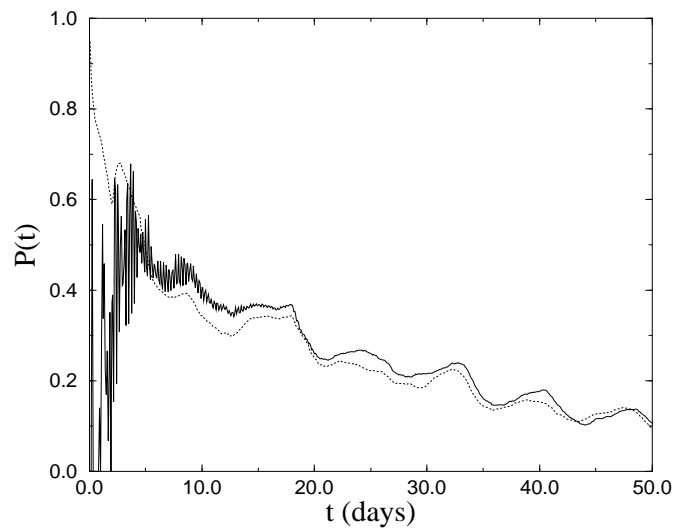


Figure 10: Time behavior of $\tilde{P}(t)$ for PE (thin curve) and SBE (dotted curve) models.

F_1	$\lambda_1(days^{-1})$	$\mu(days^{-1})$	μ/λ_1	Predictability (<i>days</i>)
0.1	6.3×10^{-2}	2.5×10^{-2}	0.4	13.2
0.25	1.7×10^{-1}	2.8×10^{-1}	1.6	3.2
0.3	4.2×10^{-1}	3.1×10^{-1}	0.7	1.7

Table 1: Maximum Lyapunov exponent λ_1 , intermittency μ , their ratio μ/λ_1 and predictability for the PE model for different values of the forcing parameter.

Models	$\lambda_1(days^{-1})$	$\mu(days^{-1})$	μ/λ_1	Predictability (<i>days</i>)
PE	6.3×10^{-2}	2.5×10^{-2}	0.4	13.2
SBE	6.5×10^{-2}	2.0×10^{-2}	0.3	13.3

Table 2: Maximum Lyapunov exponent λ_1 , intermittency μ , their ratio μ/λ_1 and predictability for the PE and SBE models at $F_1 = 0.1$.